Calculation of the apparent heat capacity in scanning calorimetry experiments on fluid phase equilibria

Ulrich K. Deiters

Institute of Physical Chemistry, University of Cologne

Abstract

Equations of state can be used not only for the calculation of fluid phase equilibria, but also for the prediction of the accompanying changes of the internal energy or enthalpy. In this work, traces of DSC (differential scanning calorimetry) or transitiometry experiments on some fluid model systems at high pressures are simulated and discussed.

keywords: transitiometry; differential scanning calorimetry; fluid phase equilibria; apparent heat capacity; retrograde behaviour; equation of state

1 Introduction

Nowadays, differential scanning calorimetry (DSC) is one of the standard methods for the determination of phase equilibria. In the majority of cases, DSC is applied at ambient pressure. But high-pressure applications are possible, too, and have already a long history; for example, Kamphausen and Schneider developed a DSC apparatus capable of reaching 250 MPa already in 1978. The design of the sample holders in this work, however, restricted the application to phase equilibria accompanied by small volume changes only, e.g., melting transitions of pure solids or structure changes of liquid crystals.

This restriction is overcome by transitiometry, which can be regarded as the logical extension of the DSC principle. The core of a transitiometer is a pair of high-pressure vessels, each one equipped with heaters and transducers for pressure, temperature as well as heat flow, and each one operated by a computer-controlled screw press [1]. A transitiometer is capable of performing isobaric temperature scans and to record the resulting heat flow like a DSC instrument, but can also do isochoric temperature scans, isothermal pressure scans, or follow arbitrary thermodynamic paths. Most important in the context of this work is that a transitiometer can accommodate volume changes large enough to make it applicable to supercritical fluids. So Bessieres *et al.* demonstrated that it could be used to determine Joule–Thomson inversion curves [2]. Baitalow *et al.* used transitiometry and DSC to study the decomposition reaction of borazane at high pressures [3].

Particularly interesting is the application of transitiometry to phase equilibria of mixtures at elevated pressure. Examples are the determination of the phase diagrams of {methane + eicosane} and {carbon dioxide + caffeine} [4], which involved solid–solid as well as solid–fluid phase equilibria.

Especially for mixtures, however, the interpretation of DSC or transitiometer traces can get rather difficult. In this work, we attempt a "transitiometer simulation", a theoretical study of the heat flow to or from the sample vessel of a transitiometer containing a binary fluid mixture. The phase equilibria inside the vessel are modeled with an equation of state. Simulations of this kind have been made before [4] for systems involving solid–fluid phase equilibria, but only with the intention to reproduce given experimental data and conditions. We furthermore acknowledge the work of Filippov and Chernik [5–7], who analyzed DTA and DSC traces of heterogenous systems, although not with equations of state nor under supercritical conditions. Here we will consider fluid-phase equilibria of some model systems, show some typical peak shapes, and discuss some counter-intuitive results.

2 Theory

2.1 The DSC/transitiometer working equations

During a scanning experiment, a DSC apparatus or transitiometer enforces a temperature or pressure change of the sample and records the resulting heat flow. We now assume an ideal instrument, which has an infinite internal heat conductivity and no internal temperature gradient, and in which the sample is always in an equilibrium state. Using the 2nd Law of thermodynamics, we can then write

$$\dot{q} = T\mathrm{d}\dot{S} \,, \tag{1}$$

where $\dot{q}$ is the absorbed or liberated heat and $\dot{S}$ the entropy production at the temperature T. Introducing the total differential of the entropy leads to

$$\dot{q} = \frac{T}{\mathrm{d}t}\left[\left(\frac{\partial S}{\partial T}\right)_V \mathrm{d}T + \left(\frac{\partial S}{\partial V}\right)_T \mathrm{d}V\right] = T\left[\frac{C_V}{T}\dot{T} + \left(\frac{\partial p}{\partial T}\right)_V \dot{V}\right] \,. \tag{2}$$

$\dot{T}$ and $\dot{V}$ are the heating and expansion rates, respectively.

For a non-isothermal scanning mode, $\dot{T} \neq 0$, we can then write

$$\dot{q} = \dot{T}\left[C_V + T\left(\frac{\partial p}{\partial T}\right)_V \frac{\mathrm{d}V}{\mathrm{d}T}\right] \,. \tag{3}$$

In the case of an isochoric scan, $\mathrm{d}V/\mathrm{d}T = 0$, and hence the heat flow becomes $\dot{q} = \dot{T}C_V$. For an isobaric scan we must set $\mathrm{d}V/\mathrm{d}T = (\partial V/\partial T)_p$, and then the resulting heat flow is

$$\dot{q} = \dot{T}\left[C_V + T\left(\frac{\partial p}{\partial T}\right)_V \left(\frac{\partial V}{\partial T}\right)_p\right] = \dot{T}\left[C_V - T\frac{\left(\frac{\partial V}{\partial T}\right)_p^2}{\left(\frac{\partial V}{\partial p}\right)_T}\right] \,. \tag{4}$$

With the common definitions of the isothermal compressibility, κ_T, and the isobaric expansivity, α_p, the result

$$\dot{q} = \dot{T}\left[C_V + \frac{TV\alpha_p^2}{\kappa_T}\right] = \dot{T}C_p \tag{5}$$

is obtained. This is the well-known working equation of (isobaric) DSC instruments. In the case of a transitiometer in "free-style mode", however, $V(T)$ and hence $\mathrm{d}V/\mathrm{d}T$ are set by the operator; then Eq. (3) must be used.

Using the total differential of $S(p,T)$ instead of $S(V,T)$ in Eq. (2) results in

$$\dot{q} = \frac{T}{\mathrm{d}t}\left[\left(\frac{\partial S}{\partial T}\right)_p \mathrm{d}T + \left(\frac{\partial S}{\partial p}\right)_T \mathrm{d}p\right] = T\left[\frac{C_p}{T}\dot{T} - \left(\frac{\partial V}{\partial T}\right)_p \dot{p}\right] \,, \tag{6}$$

which is the general working equation under (p,T) control. Division by the temperature rate and substitution of the definition of the isothermal expansivity then yields

$$\dot{q} = \dot{T}\left[C_p - TV\alpha_p\frac{\mathrm{d}p}{\mathrm{d}T}\right] \,. \tag{7}$$

For isobaric operation, $\mathrm{d}p/\mathrm{d}T = 0$, and Eq. (5) is recovered.

A transitiometer is also capable of doing pressure scans at constant temperature. For this application, Eq. (2) or (6) can used to obtain

$$\dot{q} = T\left(\frac{\partial p}{\partial T}\right)_V \dot{V} = T\left(\frac{\partial p}{\partial T}\right)_V \left(\frac{\partial V}{\partial p}\right)_T \dot{p} = -TV\alpha_p \dot{p} \tag{8}$$

which is the working equation for a transitiometer in isothermal mode.

The thermodynamic energy function associated with $\dot{q}$ is

$$E = \int \dot{q}\,\mathrm{d}t = \begin{cases} U & \text{isochoric} \\ H & \text{isobaric} \\ U + \int T\left(\frac{\partial p}{\partial T}\right)_V \frac{\mathrm{d}V}{\mathrm{d}T}\,\mathrm{d}T & \text{arbitrary nonisothermal path} \\ TS & \text{isothermal} \end{cases} \tag{9}$$

2.2 Heat flow in a two-phase region

Eq. (2) is true for single-phase systems[1]. For two-phase states, the entropy contributions of both phases have to be added:

$$S = n' S'_\mathrm{m} + n'' S''_\mathrm{m} \tag{10}$$

The amounts of substance in the two phases, n' and n'', can be obtained from the "lever rule", which for a two-component system is

$$n'(x'_1 - x_1) + n''(x''_1 - x_1) = 0\ . \tag{11}$$

Here x'_1 and x''_1 are the equilibrium mole fractions, and x_1 the overall mole fraction of the system. Rearrangement yields

$$\begin{aligned} n' &= nf' \quad \text{with } f' = \frac{x''_1 - x_1}{x''_1 - x'_1} \\ n'' &= nf'' \quad \text{with } f'' = \frac{x_1 - x'_1}{x''_1 - x'_1}\ , \end{aligned} \tag{12}$$

where f' and f'' are the phase fractions. For multicomponent systems similar, although slightly more complicated equations can be obtained.

Differentiation of Eq. (10), noting that the equilibrium mole fractions as well as the entropies generally depend on temperature, results in

$$\begin{aligned} \dot{q} =& n\dot{T}\Bigg[\left(C'_\mathrm{m} f' + C''_\mathrm{m} f''\right) \\ &+ T\left(\left(\frac{\mathrm{d}S'_\mathrm{m}}{\mathrm{d}x'_1} - \frac{S''_\mathrm{m} - S'_\mathrm{m}}{x''_1 - x'_1}\right)\frac{\mathrm{d}x'_1}{\mathrm{d}T} f' + \left(\frac{\mathrm{d}S''_\mathrm{m}}{\mathrm{d}x''_1} - \frac{S''_\mathrm{m} - S'_\mathrm{m}}{x''_1 - x'_1}\right)\frac{\mathrm{d}x''_1}{\mathrm{d}T} f''\right)\Bigg]\ . \end{aligned} \tag{13}$$

The heat capacities C_m, the entropy derivatives $\mathrm{d}S_\mathrm{m}/\mathrm{d}x_1$, and the mole fraction derivatives $\mathrm{d}x_1/\mathrm{d}T$ must be taken in accordance with the thermodynamic path of the calorimeter. For an

[1] more accurately: for systems where the amounts of the components in each phase do not change

isobaric experiment, they latter are the slopes of the phase boundary curves in a conventional isobaric Tx phase diagram. Then this equation can be written as

$$\begin{aligned}\dot{q} =& n\dot{T}\Bigg[\left(C'_{p\mathrm{m}} f' + C''_{p\mathrm{m}} f''\right) \\ &+ T\left(\left(\left(\frac{\partial S'_\mathrm{m}}{\partial x'_1}\right)_{p,T} - \frac{S''_\mathrm{m} - S'_\mathrm{m}}{x''_1 - x'_1}\right)\frac{\mathrm{d}x'_1}{\mathrm{d}T} f' + \left(\left(\frac{\partial S''_\mathrm{m}}{\partial x''_1}\right)_{p,T} - \frac{S''_\mathrm{m} - S'_\mathrm{m}}{x''_1 - x'_1}\right)\frac{\mathrm{d}x''_1}{\mathrm{d}T} f''\right)\Bigg] .\end{aligned} \tag{14}$$

Combination of this equation with the isobaric Gibbs–Konowalow equations,

$$\frac{\mathrm{d}x'_1}{\mathrm{d}T} = \left(\left(\frac{\partial S'_\mathrm{m}}{\partial x_1}\right)_{p,T} - \frac{S''_\mathrm{m} - S'_\mathrm{m}}{x''_1 - x'_1}\right)\frac{1}{G'_{2x}} . \tag{15}$$

and its analogue for $\mathrm{d}x''_1/\mathrm{d}T$, leads to the result of Filippov and Chernik [5–7]:

$$\dot{q} = n\dot{T}\left[\left(C'_{p\mathrm{m}} f' + C''_{p\mathrm{m}} f''\right) + T\left(\left(\frac{\mathrm{d}x'_1}{\mathrm{d}T}\right)^2 G'_{2x} f' + \left(\frac{\mathrm{d}x''_1}{\mathrm{d}T}\right)^2 G''_{2x} f''\right)\right] . \tag{16}$$

Here G_{2x} is a shorthand notation for $(\partial^2 G_\mathrm{m}/\partial x_1^2)_{p,T}$, the 2nd order derivative of the molar Gibbs energy with respect to mole fraction. For a stable phase, $G_{2x} > 0$ must be true (diffusion stability).

Let us assume that the sample passes from a single-phase state through a two-phase region to another single-phase state; an example is the evaporation of a liquid, l→lg→g. The heat flow of the calorimeter is $n\dot{T}C'_{p\mathrm{m}}$ before the transition and $n\dot{T}C''_{p\mathrm{m}}$ afterwards (identifying phase ′ with the liquid and ″ with the gas phase). Evidently, the first term within the angular brackets of Eq. (16) is a linear interpolation between C'_m and C''_m, and it can be represented in the calorimeter traces by smooth connection of the baselines before and after the transition. The second term within contains the 2nd order derivatives of the Gibbs energy with respect to the mole fractions — which must be positive for stable phases — and the squares of the slopes of the phase envelopes. This term cannot be negative; it therefore increases the apparent heat capacity within the two-phase region.

For isochoric or other thermodynamic paths, the derivatives $\mathrm{d}S_\mathrm{m}/\mathrm{d}x_1$ and $\mathrm{d}x_1/\mathrm{d}T$ also reflect the pressure influence on the phase boundaries. In this case, the simplification by means of the the Gibbs–Konowalow equation is no longer possible (or leads to additional terms). But it is not really necessary to calculate the working function analytically. For practical purposes, numerical differentiation of Eq. (10) is preferable.

2.3 Equation of state

For a discussion of the qualitative features of DSC or transitiometer traces, accurate numerical results are not really needed. We therefore base our calculations on a simple, cubic equation of state, namely the equation of Peng and Robinson [8], which we write here in the form

$$\begin{aligned} Z = \frac{pV_\mathrm{m}}{RT} &= \frac{1}{1-\xi} - \frac{8\xi\alpha(\tilde{T})}{(1+2\xi-\xi^2)\tilde{T}} \\ \text{with } \xi = \frac{v^*}{V_\mathrm{m}} \qquad \tilde{T} &= \frac{T}{T^*} \\ \text{and } \alpha(\tilde{T},\omega) &= \left[1 + m(\omega)\left(1 - \sqrt{\frac{\tilde{T}}{\tilde{T}_\mathrm{c}}}\right)\right]^2 . \end{aligned} \tag{17}$$

Here ξ and $\tilde{T}$ are the reduced density and the reduced temperature respectively, v^* the characteristic volume (covolume), T^* the characteristic temperature, and $m(\omega)$ a polynomial of the acentric factor. The commonly used attraction parameter of this equation of state is $a_{\mathrm{PR}} = 8RT^*v^*\alpha(\tilde{T},\omega)$. The reduced critical temperature is a constant, $\tilde{T}_{\mathrm{c}} = 1.361155$.

For mixtures we use Soave's mixing rules [9]:

$$(T^*v^*) = \sum_{i=1}^{N}\sum_{j=1}^{N} x_i x_j v_{ij}^* T_{ij}^* \sqrt{\alpha(\tilde{T}_{ii},\omega_i)\alpha(\tilde{T}_{jj},\omega_j)} \tag{18}$$

$$v^* = \sum_{i=1}^{N} x_i v_{ii}^* \tag{19}$$

The T_{ij}^* (with $i \neq j$) are adjustable parameters of the mixture.

From these equations, the required thermodynamic energy functions and heat capacities can be obtained by means of well-known thermodynamic relations. So the residual molar Helmholtz energy, internal energy, and isochoric heat capacity are

$$\frac{A_{\mathrm{m}}^{\mathrm{r}}}{RT} = \int_0^{\xi} \frac{Z-1}{\xi}\,\mathrm{d}\xi \tag{20}$$

$$\frac{U_{\mathrm{m}}^{\mathrm{r}}}{RT} = -T\left(\frac{\partial A_{\mathrm{m}}^{\mathrm{r}}/RT}{\partial T}\right)_{V_{\mathrm{m}}} \tag{21}$$

$$\frac{C_{V\mathrm{m}}^{\mathrm{r}}}{R} = 2\frac{U_{\mathrm{m}}^{\mathrm{r}}}{RT} - T^2\left(\frac{\partial^2(A_{\mathrm{m}}^{\mathrm{r}}/RT)}{\partial T^2}\right) \ . \tag{22}$$

For the total heat capacity, the ideal-gas heat capacity, $C_{V\mathrm{m}}^{\mathrm{id}}(T)$ has to be added:

$$C_{V\mathrm{m}}^{\mathrm{id}}(T) = C_{p\mathrm{m}}^{\mathrm{id}}(T) - R = \sum_{i=1}^{N} x_i C_{p\mathrm{m},i}(T) - R \tag{23}$$

The isobaric ideal-gas heat capacities of the pure components, $C_{p\mathrm{m},i}^{\mathrm{id}}(T)$, can be conveniently obtained by spline extrapolations of tables of experimental data.

Calculations of phase envelopes, critical curves, and apparent heat capacities were performed with the *ThermoC* program package, where the equations of this Section are implemented [10].

3 Application to high-pressure fluid phase equilibria

For simplicity's sake we will discuss heating runs of calorimetric experiments only, so that $\dot{T} > 0$; absorption of heat by the sample then corresponds to $\dot{q} > 0$.

3.1 Example: {methane + propane}

The fluid mixture {methane + propane} has a rather simple phase diagram, in which only one critical curve appears (Fig. 1) [11]. Its phase diagram belongs to class I according to the system of van Konynenburg and Scott [12], or 1^P according to the rational nomenclature of Bolz *et al.* [13]. The critical curve passes through a pronounced pressure maximum, which is common for this type of mixtures.

A subcritical isobaric Tx cross section, Fig. 2, exhibits the typical spindle-shaped vapour–liquid coexistence region. Because of Eq. (16), the phase separation causes a positive contribution to $\dot{q}$. Fig. 3 shows a positive peak in the two-phase region, with two spikes marking the passing of the bubble point curve (l→lg) and the dew point curve (lg→l).

At pressures above the critical pressures of both pure components, the Tx phase envelope detaches from the ordinates of the phase diagram and develops two binary critical points, as shown in Fig. 4. The maximum of the critical curve in Fig. 1 is a so-called elliptic critical pressure maximum [13]; here the two-phase region contracts to a point and vanishes. In the vicinity of the binary critical points in Fig. 4 retrograde behaviour occurs, and one of the phase boundaries has a positive slope. Still, as only the squares of the slopes appear in the isobaric working function Eq. (16), the two-phase region always shows a higher apparent heat capacity than the single phase region (Fig. 5).

If the phase separation is delayed until the phase becomes unstable ($G_{2x} < 0$), it is possible to have negative spikes. This is probably not a realistic option for {methane + propane} mixtures, but can be easily arranged on a computer. For viscous polymer mixtures, however, "spinodal decomposition" (delayed phase separation on reaching $G_{2x} = 0$) has been experimentally observed. For such systems, negative DSC signals are therefore possible.

In DSC or transitiometry experiments the baseline is usually suppressed or at least displaced by subtracting the signal of the reference cell. Then a negative peak might look "wrong", i.e., be mistaken for an exothermic transition during a heating run, or an endothermic transition during a cooling run. It should be noted, however, that Fig. 5 shows the *total* apparent heat capacity still to be positive.

Another interesting feature of Fig. 5 is the pronounced maximum of the baseline, which might be, at a first glance, mistaken for a signature of a phase separation. This maximum, however, is relatively broad, whereas the spikes, the true indicators of phase boundaries, are rather sharp.

The traces of *isochoric* transitiometer runs are similar to their isobaric counterparts. Some points, however, need to be considered:

- If an isochoric run were to start at low temperature with a liquid mixture, the thermal expansion during heating would drive the pressure quickly to more than 100 MPa, and no vapour–liquid equilibrium would ever occur.
- But if, at the begin of the run, the sample is already in a two-phase state and has a total volume larger than the its critical volume, an experimental path like curve C in Fig. 1 results. The sample changes from a two-phase to a single-phase vapour state (lg→g) when curve C crosses the isopleth, i.e., the liquid evaporates. As the entropy term in Eq. (13) disappears, a negative step results in the transitiometer trace (Fig. 6).

  The underlying principle — an increased apparent heat capacity in the two-phase region — is the same as for Fig. 3. But as the bubble point branch of the isopleth (l→lg) is never crossed during the isochoric run, the ascending part of the peak does not appear: the peak, the signal of the two-phase region, extends all the way from the begin of the run to the negative step and is (because of its width) usually not very high, so that it can easily be mistaken for the baseline.
- If the run starts with a two-phase state having a total molar volume less than the critical volume, the gas phase condenses completely when the isopleth is crossed (lg→l). This case corresponds to curve D in Fig. 1. One might intuitively expect a negative heat flow, for condensation is an exothermic process. But again, the apparent heat capacity is higher in the two-phase region than in the single-phase region, and hence a single negative step results.

Figs. 7 and 8 show an isothermal phase diagram and isothermal transitiometer traces, respectively, at a temperature where methane is supercritical. For a methane mole fraction of 0.2, the transitiometer trace shows the usual increased apparent heat capacity in the two-phase region, with two spikes marking the crossing of the phase boundaries. At the mole fraction 0.55, retrogade behaviour occurs, and now one of the spikes is negative.

3.2 Example {carbon dioxide + hexadecane}

Fig. 9 shows the pT phase diagram of a binary mixture whose parameters were set as to approximately mimic {carbon dioxide + hexadecane}.[2] The diagram belongs to class $\mathrm{III_m}$ (rational momenclature $1^C W 1^Z$) [14, 15]; it exhibits a pressure maximum and a minimum along the critical curve which originates at the less volatile component. The maximum is an elliptic critical pressure maximum; here the phase diagram topology and the transitiometer traces are similar to the ones of the {methane + propane} system. The minimum is a hyperbolic critical pressure minimum [13]; here two two-phase regions merge and form a band of limited miscibility.

Fig. 10 contains an isobaric Tx cross section just below the critical pressure minimum, and through the small l=g critical curve originating at the critical point of carbon dioxide. Transitiometer traces in the vicinity of the band-like liquid–liquid 2-phase region show only rather small spikes at the phase boundaries, and also a very small baseline shift, which is not surprising: The energy term in Eq. (13) contains the factors $\mathrm{d}x_1'/\mathrm{d}T$ and $\mathrm{d}x_1''/\mathrm{d}T$, which both vanish at the "waistline" of the two-phase region. In fact, a transitiometer run taking a path through the two-phase region would register the heat capacity term only.

The dominant features of the transitiometer traces are the huge spikes caused by crossing the three-phase curve llg. The phase state of the sample changes here according to $\mathrm{l_1l_2} \rightarrow \mathrm{l_1l_2g} \rightarrow \mathrm{l_1g}$ This amounts to the evaporation of a liquid at the temperature of the three-phase state, and consequently the transitiometer traces contain a large, sharp spike similar to the evaporation peak of a pure liquid.

4 Conclusions

Even if only fluid phase equilibria are considered and complications due to the existence of solid phases neglected, the resulting traces of scanning-calorimetry experiments — DSC or transitiometry — can exhibit an interesting variety of shapes. Due to the appearance of an additional term (the energy contribution) in the equation for the apparent heat capacity, this property usually has a higher value in two-phase regions than in single-phase regions.

Isochoric transitiometer runs on mixtures with high-pressure vapour–liquid equilibria typically result in very broad and low signals. Here often only a negative step is conspicuous, which marks the transition to a single-phase state.

In regions of retrograde behaviour, isothermal transitiometer runs may exhibit "negative signals".

Of course, simulations of scanning calorimetry runs by means of equations of state cannot be substitutes for the experiments, but they can facilitate the interpretation of calorimetric signals and the construction of phase diagrams.

[2] It is not possible to accurately represent this mixture with Eqs. 17–19. With parameters chosen to represent the high-pressure part of the major critical curve well, its minimum is somewhat too deep in comparison with experimental data — which, however, scatter considerably.

Acknowledgments
We wish to thank Dr. S. L. Randzio (Polish Academy of Sciences, Warsaw) for bringing the problem to our attention.

Symbols

A	Helmholtz energy
C	heat capacity
E	generalized energy function
f	phase fraction
G	Gibbs energy
H	enthalpy
n	amount of substance, "number of moles"
p	pressure
q	heat
R	universal gas constant
S	entropy
T	temperature
t	time
U	internal energy
V	volume
x	mole fraction
Z	compression factor, $Z = pV/(nRT)$
α_p	isobaric thermal expansivity
κ_T	isothermal compressibility

Subscripts

i	related to component i
m	molar property
p	derivative at constant pressure
V	derivative at constant volume

Superscripts

id	ideal-gas property
r	residual property
$'$,$''$	phase indicators
*	characteristic property (parameter of an equation of state)

References

[1] S. L. Randzio, Chem. Soc. Rev. 25 (1996) 383–392.

[2] D. Bessieres, S. L. Randzio, M. M. Piñeiro, Th. Lafitte, and J.-L. Daridon, J. Phys. Chem. B 110 (2006) 5659–5664.

[3] F. Baitalow, G. Wolf, J. P. E. Grolier, F. Dan, and S. L. Randzio, Thermochim. Acta 445 (2006) 121–125.

[4] U. K. Deiters and S. L. Randzio, Fluid Phase Equilib. 260 (2007) 87–97.

[5] V. K. Filippov, Dokl. Akad. Nauk SSSR 242 (1978) 376–379.

[6] V. K. Filippov and G. G. Chernik, Thermochim. Acta 101 (1986) 65–75.

[7] G. G. Chernik, J. Coll. Interface Sci. 141 (1991) 400–408.

[8] D. Y. Peng and D. B. Robinson, Ind. Eng. Chem. Fundam. 15 (1976) 59–64.

[9] G. Soave, Chem. Eng. Sci. 27 (1972) 1197–1203.

[10] U. K. Deiters. *ThermoC* project homepage: http://thermoc.uni-koeln.de/index.html.

[11] H. H. Reamer, B. H. Sage, and W. N. Lacey, Ind. Eng. Chem. 42 (1950) 534–539.

[12] P. H. van Konynenburg and R. L. Scott, Phil. Trans. R. Soc. Lond. A 298 (1980) 495–540.

[13] A. Bolz, U. K. Deiters, C. J. Peters, and Th. W. de Loos, Pure Appl. Chem. 70 (1998) 2233–2257.

[14] G. Schneider, Ber. Bunsenges. Phys. Chem. 70 (1966) 10–16.

[15] T. Charoensombutamon, R. J. Martin, and R. Kobayashi, Fluid Phase Equilib. 31 (1986) 89–104.

Figure captions

Fig. 1: Phase diagram of the {methane + propane} system, calculated with the Peng–Robinson equation of state. —: vapour pressure curves, ○: pure-component critical points, **—**: critical curve, - - -: isopleth $x_1 = 0.4$,·····: paths of transitiometer runs (A: isobaric, Fig. 2–3; B: isobaric, Fig. 4)–5; C, D: isochoric, Fig. 6), E: isothermal, Fig. **??**.

Fig. 2: Isobaric phase diagram of the {methane(1) + propane(2)} system at 1 MPa, calculated with the Peng–Robinson equation of state. The arrow indicates the path of a transitiometer run for a sample with the overall mole fraction $x_1 = 0.5$ (Fig. 3).

Fig. 3: Simulated trace of a transitiometer for a {methane(1) + propane(2)} sample with the overall composition x_1 = 0.5 at 1 MPa.

Fig. 4: Isobaric phase diagram of the {methane(1) + propane(2)} system at 8 MPa, calculated with the Peng–Robinson equation of state. ○: binary critical points. The arrows indicate the paths of transitiometer runs (Fig. 5).

Fig. 5: Simulated traces of a transitiometer for {methane(1) + propane(2)} samples with the overall compositions x_1 = 0.4 and 0.9 at 8 MPa. Lower curve at x_1 = 0.4: phase separation delayed, after attaining diffusional instability.

Fig. 6: Simulated traces of a transitiometer for a {methane(1) + propane(2)} sample with the overall composition x_1 = 0.4 at V = 279.5 cm^3/mol (path C in Fig. 1) or 80 cm^3/mol (path D).

Fig. 7: Isothermal phase diagram of the {methane(1) + propane(2)} system at 320 K, calculated with the Peng–Robinson equation of state. ○: binary critical point. The arrows indicate the paths of transitiometer runs (Fig. 8).

Fig. 8: Simulated traces of a transitiometer for {methane(1) + propane(2)} samples with the overall compositions x_1 = 0.2 and 0.55 at 320 K.

Fig. 9: Phase diagram of a class III$_\mathrm{m}$ system. —: vapour pressure curves, ○: pure-component critical points, **—**: critical curves, –·–·: three-phase curve llg.

Fig. 10: Isobaric phase diagram of the class III$_\mathrm{m}$ system at 8 MPa. —: phase boundaries, –·–·: three-phase state. The insert shows an enlargement of the llg coexistence region; ○: binary critical point l=g. The arrows indicate the paths of transitiometer experiments (see Fig. 11).

Fig. 11: Simulated traces of transitiometer runs for the class III$_\mathrm{m}$ system with mole fractions x_1 = 0.90 and 0.92 at 8 MPa.

Figures

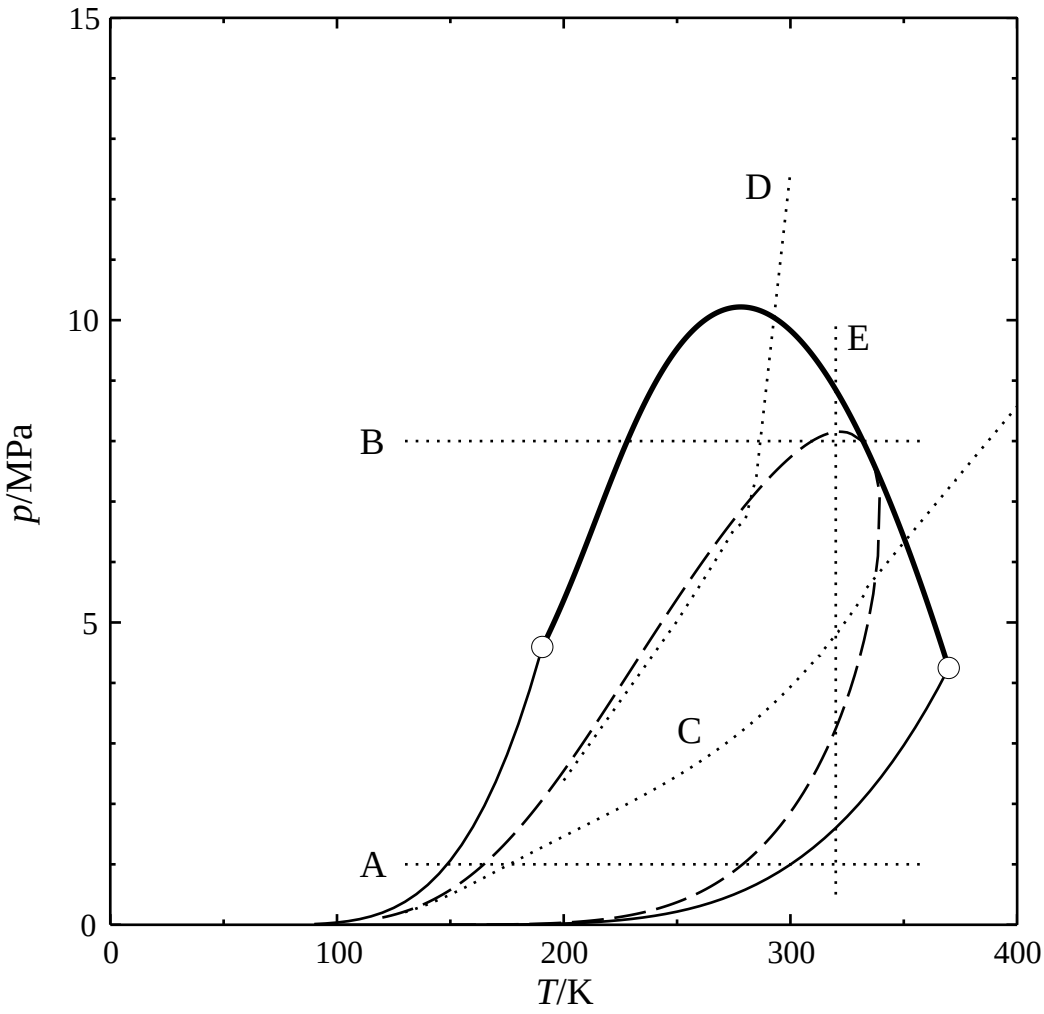

Fig. 1

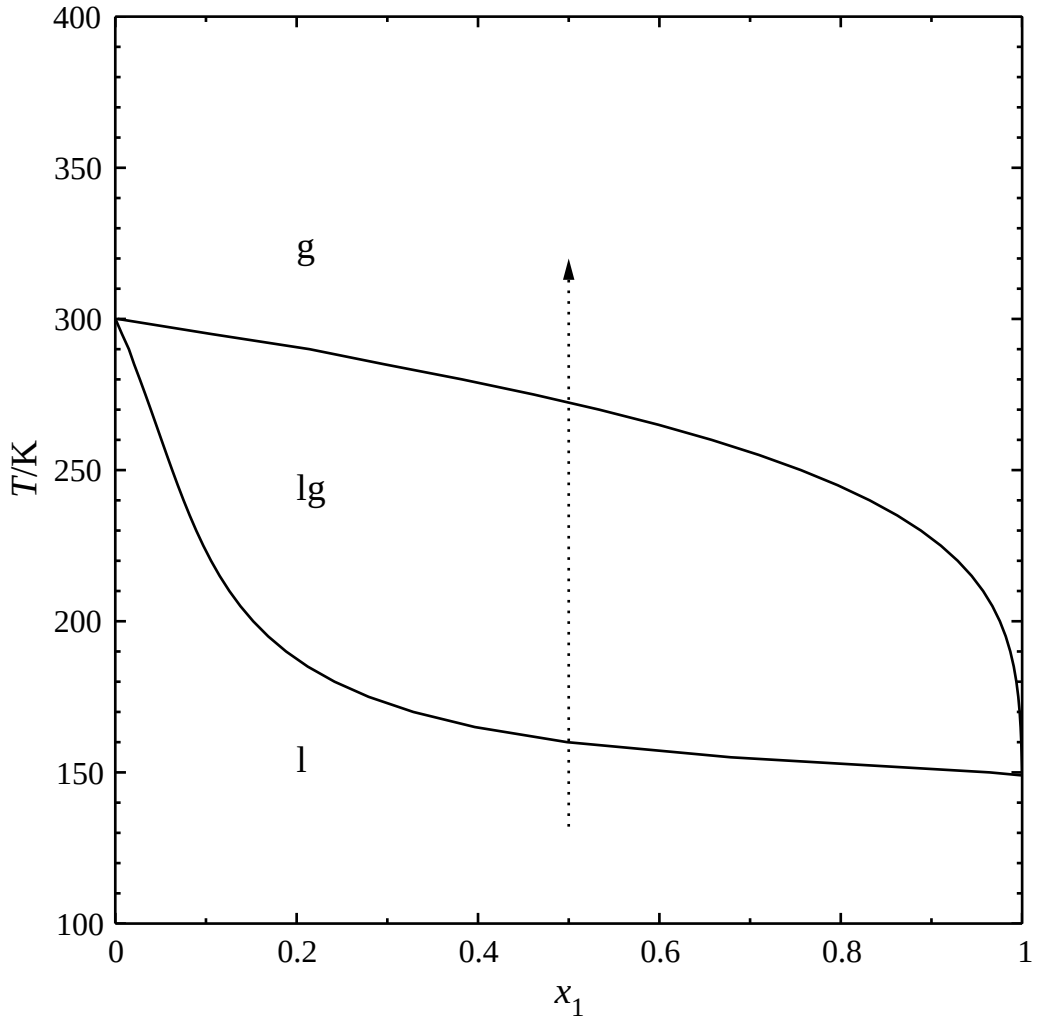

Fig. 2

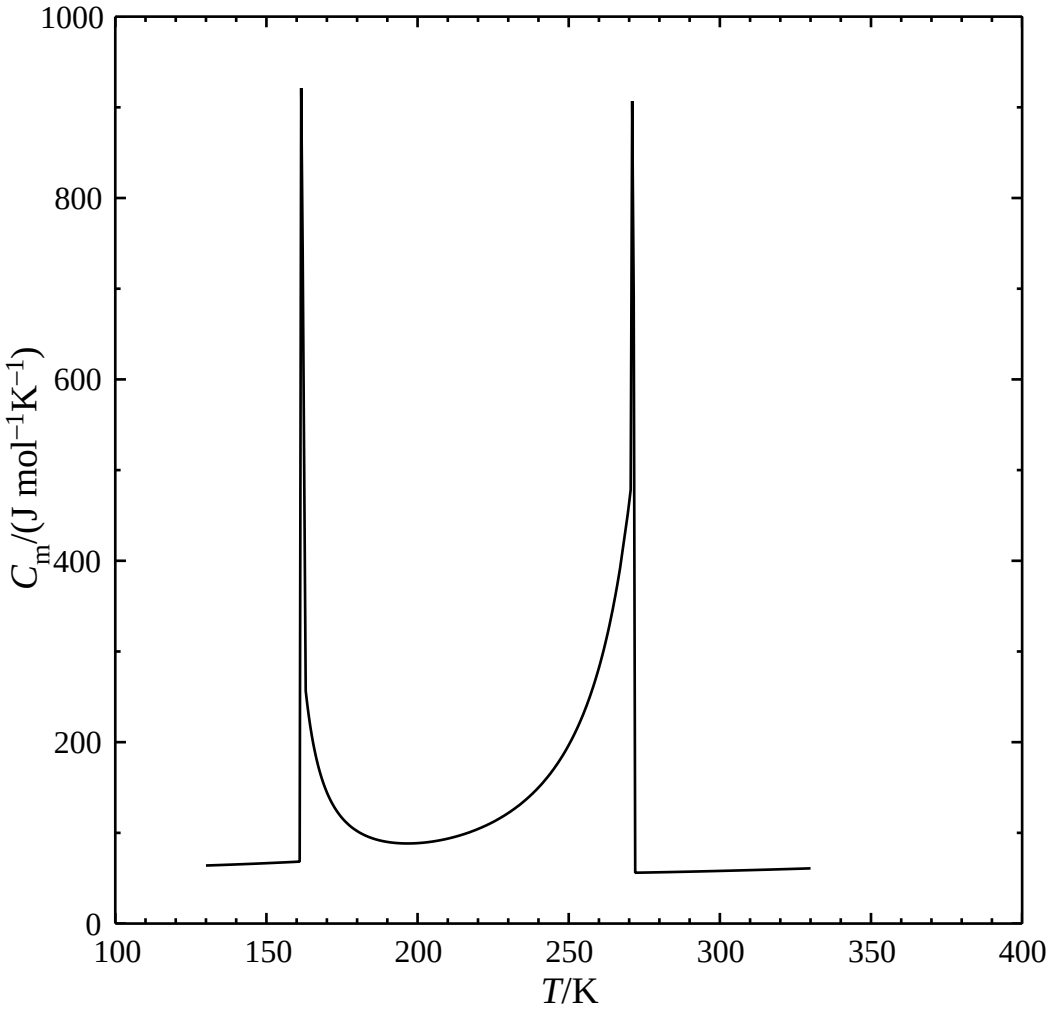

Fig. 3

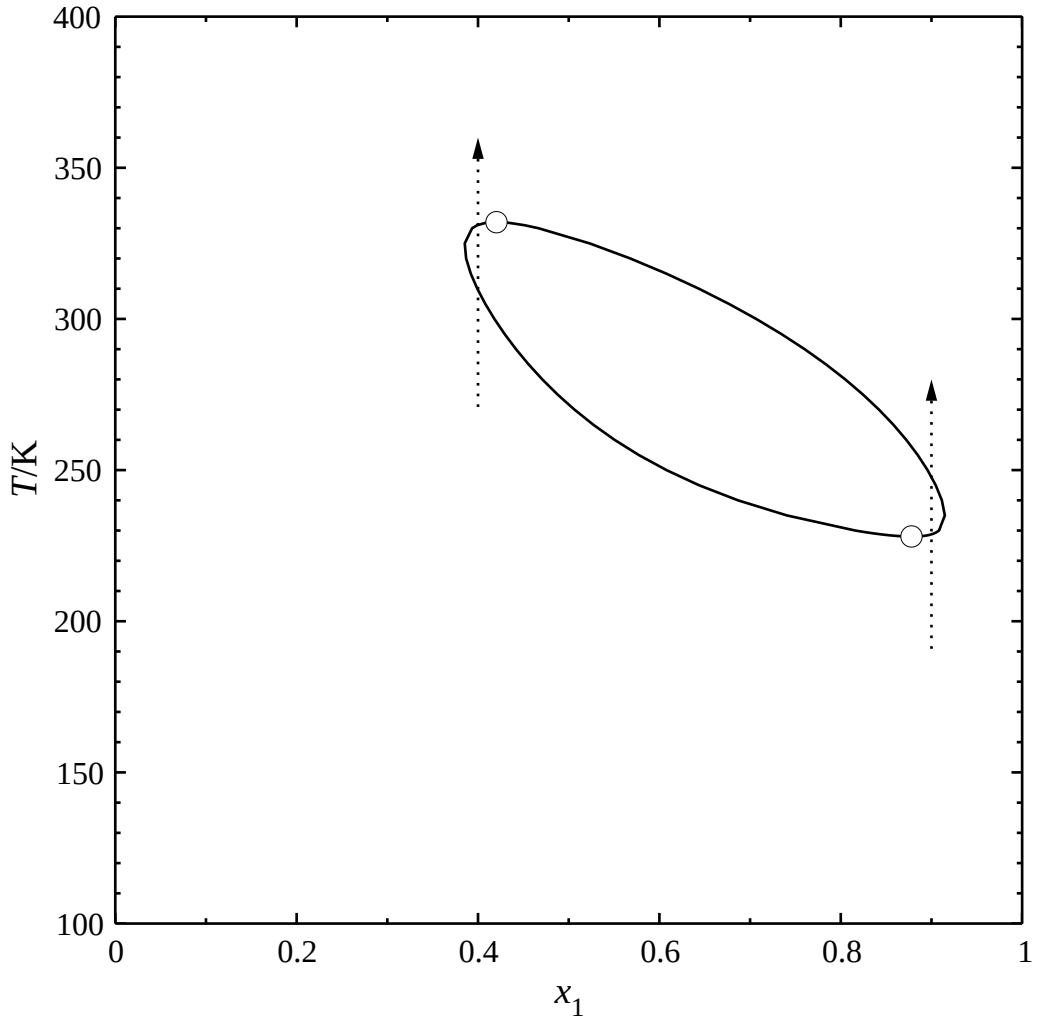

Fig. 4

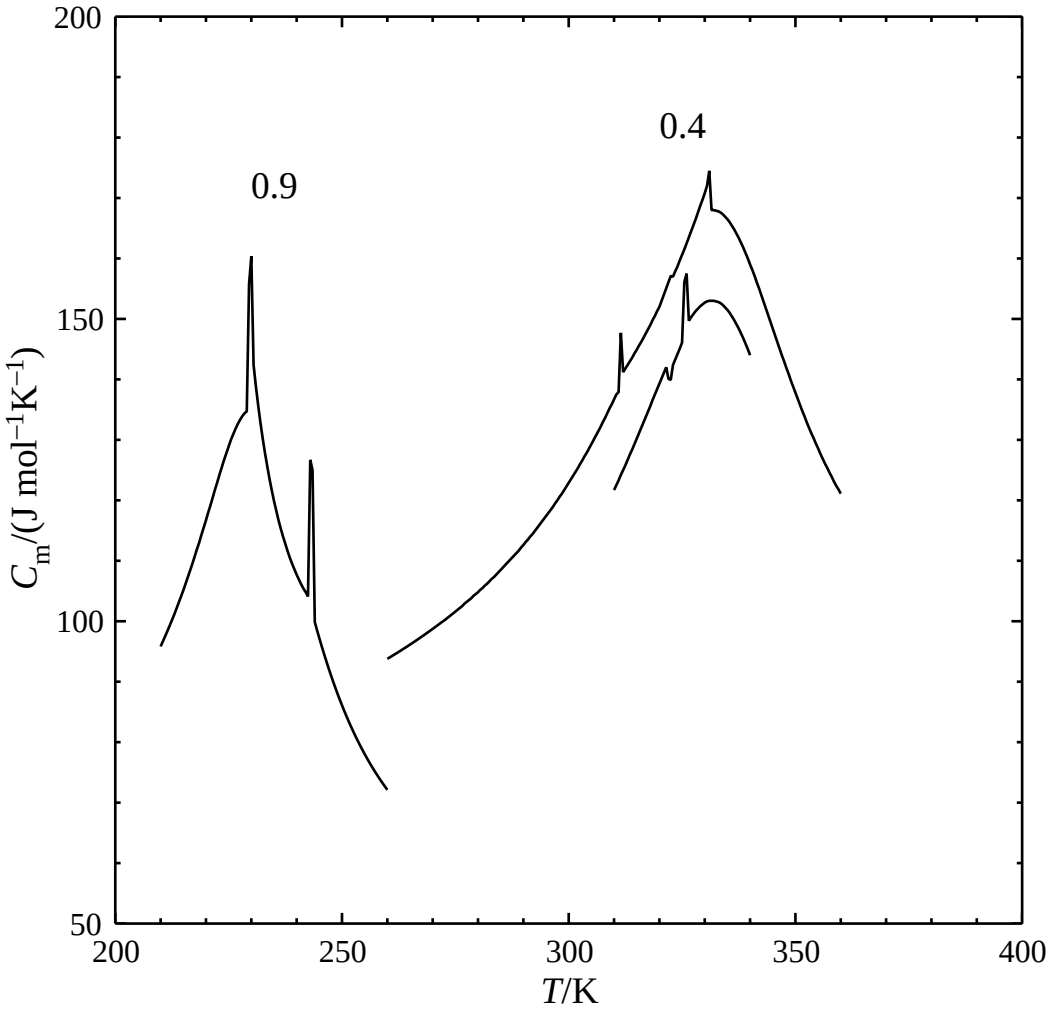

Fig. 5

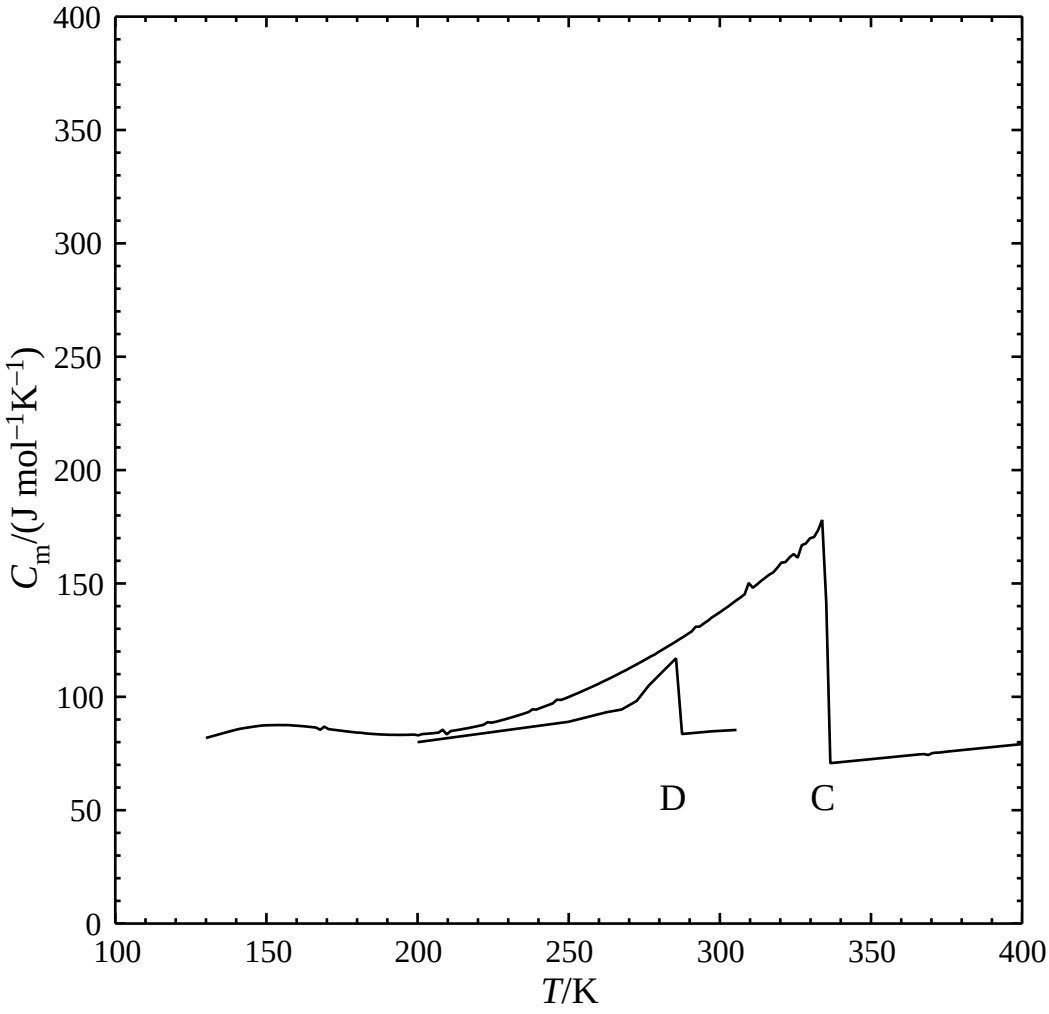
400
350
300
250
200
150
100
50
0
100
150
200
250
300
350
400
C_m/(J mol^{-1}K^{-1})
T/K
D
C

Fig. 6

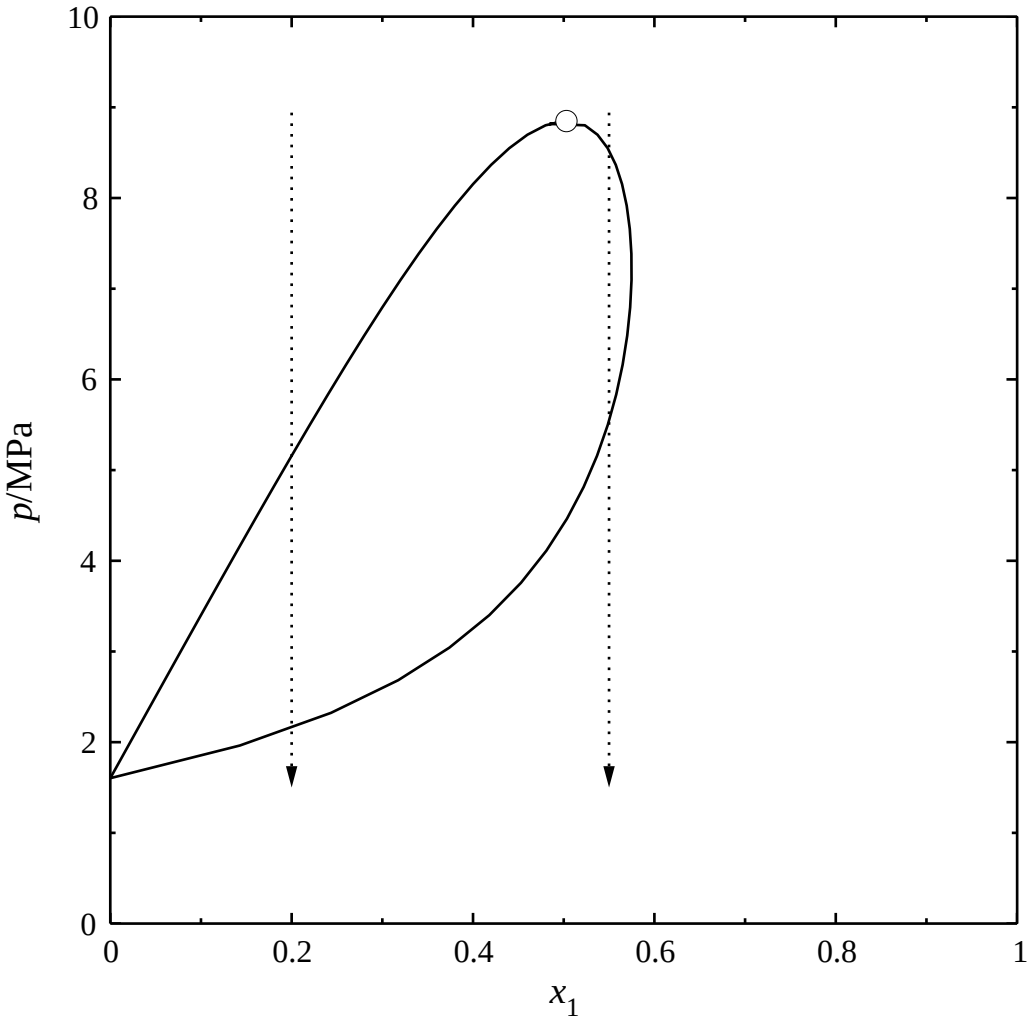

Fig. 7

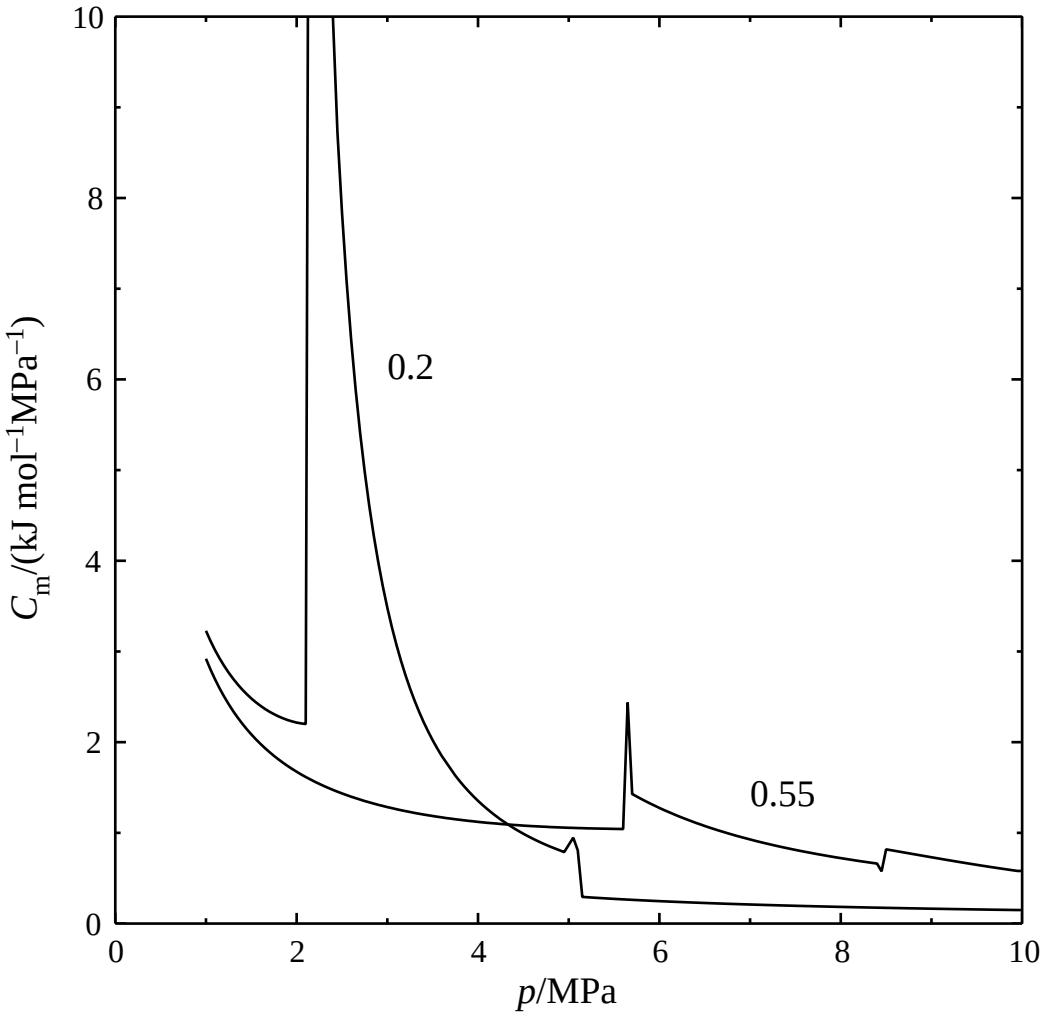

Fig. 8

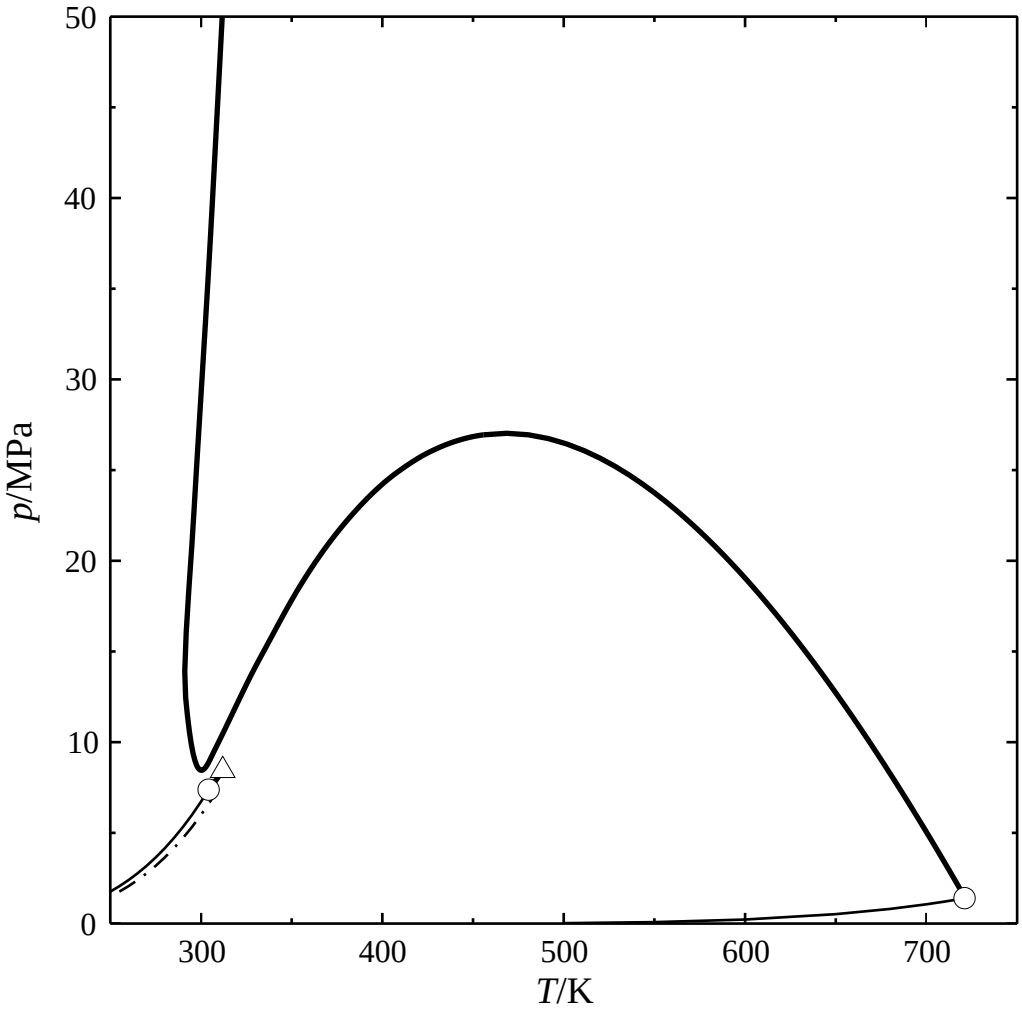

Fig. 9

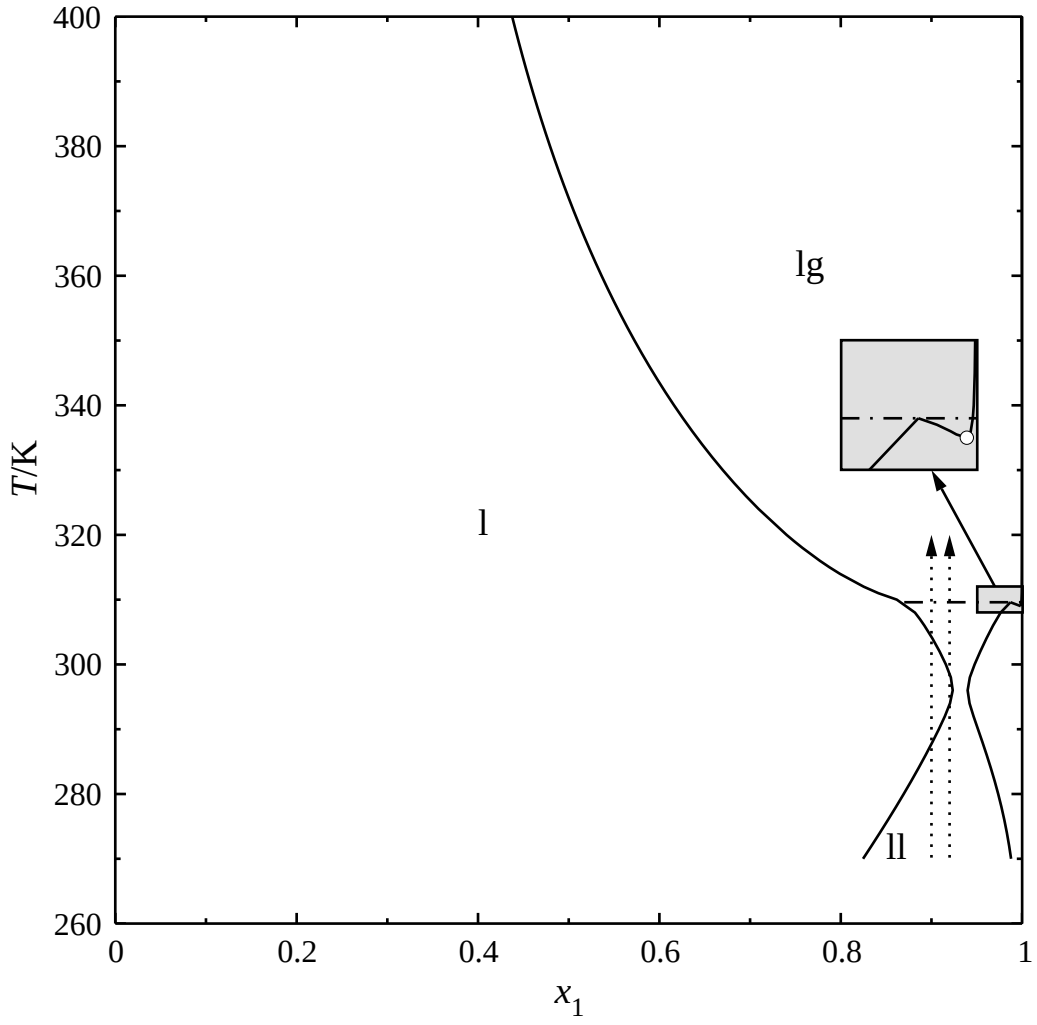

Fig. 10

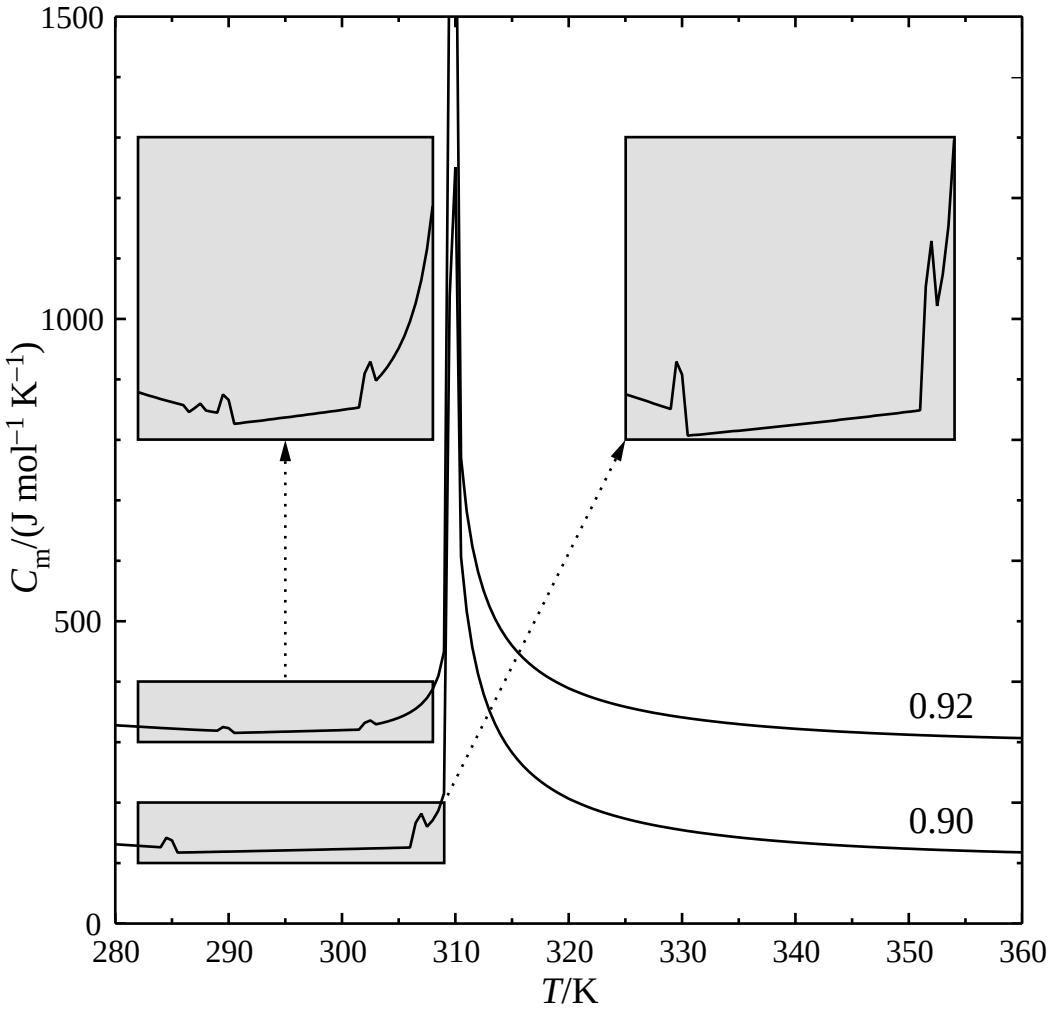
1500
1000
500
0
C_m/(J mol^{-1} K^{-1})
280
290
300
310
320
330
340
350
360
T/K
0.92
0.90

Fig. 11